

Novel fatty acid anion-based ionic liquids: contact angle, surface tension, polarity fraction and spreading parameter

D. Blanco^{a*}, N. Rivera^b, P. Oulego^c, M. Díaz^c
R. González^{b,d}, A. Hernández Battez^{a,d}

^a Department of Construction and Manufacturing Engineering, University of Oviedo, Asturias, Spain

^b Department of Marine Science and Technology, University of Oviedo, Asturias, Spain

^c Department of Chemical and Environmental Engineering, University of Oviedo, Asturias, Spain

^d Faculty of Science & Technology, Bournemouth University, UK

(*)Email: blancoadavid@uniovi.es

Abstract

This work deals with the determination of several wetting properties (contact angle, surface tension, polarity fraction and spreading parameter) of six novel fatty acid anion-based ionic liquids (FAILs): methyltrioctylammonium hexanoate $[N_{8881}][C_{6:0}]$, methyltrioctylammonium octanoate $[N_{8881}][C_{8:0}]$, methyltrioctylammonium laurate $[N_{8881}][C_{12:0}]$, methyltrioctylammonium palmitate $[N_{8881}][C_{16:0}]$, methyltrioctylammonium stearate $[N_{8881}][C_{18:0}]$ and methyltrioctylammonium oleate $[N_{8881}][C_{18:1}]$. Surface tension was determined at temperatures from 293 to 333 K, exhibiting a linear decrease **within the temperature range**. Contact angle measurements were performed on five different surfaces (steel, aluminum, tungsten carbide, cast iron and bronze) using 3 test liquids (water, diiodomethane and ethylenglycol) and each of the synthesized FAILs. Polarity fraction (PF) and the spreading parameter (SP) were calculated in order to gain a deeper understanding of wetting characteristics of these FAILs. Despite the similarity of the obtained results with all FAILs and surfaces, $[N_{8881}][C_{6:0}]$ and $[N_{8881}][C_{8:0}]$ with both cast iron and bronze surfaces were the best surface-FAIL combinations regarding wettability.

Keywords: Contact angle, fatty acid ionic liquids, polarity, spreading parameter, surface tension, wetting.

1. Introduction

Wettability of solids with liquids is a key factor for many industrial processes involving two different phases, such as catalysis, coatings and lubrication, among others. The interaction between phases affects not only the product properties, but also the nature of the engineering process [1]. Measuring several physicochemical parameters (including surface tension and contact angle) is the ideal way to start the evaluation of the wetting ability [2].

Ionic liquids (IL), salts which melting point below 100 °C, have attracted attention from both academic and industrial sectors as potential candidates for a wide variety of applications [3-14]. This mentioned interest is based on their unique properties, such as near-zero vapor pressure, high ionic conductivity, high thermal stability, large liquid range and a highly tunable solvating capacity regardless of the polarity of the compound. Therefore, the study of their physicochemical properties is important in order to use these substances in a wide range of applications [15-19]. **One of the key properties of ILs** is the fact that a small variation in the chemical

composition could drastically change their physicochemical properties, like conductivity, viscosity, melting point, density or surface tension, becoming self-tuning compounds with enormous potential in engineering applications [20, 21]. That is why, it is necessary to perform an in-depth physicochemical characterization of these substances for establishing correlations between structure and performance parameters [22, 23].

Because of the increasing research work using ionic liquids in lubrication in the last 18 years [24-29], it is important the study of key properties of these compounds, such as viscosity, density, wettability, thermal stability and tribofilm formation, which are closely related with lubrication [30-46]. Therefore, tribology research should face the knowledge of wettability parameters with the aim of getting a better design of lubrication systems [47-52]. Currently, the synthesis and use of halogen- and metal-free ionic liquids is gaining attention in order to develop more sustainable additives and lubricants. In this sense, the goal of this work is the characterization of the wetting properties (surface tension, contact angle, polarity fraction and spreading parameter) of six ionic liquids obtained from fatty acids without both halogens and metals in their composition to be used as lubricant additive.

2. Material and methods

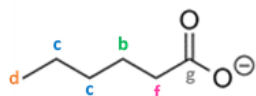
2.1 Surfaces and ionic liquids

The reagents used in the synthesis of the fatty acid ionic liquids (FAILs) include methyltrioctylammonium bromide ionic liquid ($[N_{8881}][Br]$) (> 97%) as cation precursor; hexanoic, octanoic, lauric, palmitic, stearic and oleic acids (natural > 98%) as anion precursors; sodium hydroxide, ethanol solution (70%w/w) and toluene (99.8%). All these reagents were provided by Sigma-Aldrich S.A and used without further purification. These FAILs were obtained through a salt metathesis reaction, which is explained in a previous research work [53]. The FTIR and 1H and ^{13}C NMR analyses were conducted to confirm the molecular structures of the synthesized ILs. The NMR spectra were obtained with a Bruker serie Avance AV600 nuclear magnetic resonance spectrometer (NMR) using $CDCl_3$ as the solvent. The NMR was operated with a 5 mm broad band probe at 600.15 and 150.92 MHz resonance frequencies for 1H and ^{13}C NMR, respectively. Tables 1-2 show the chemical shifts of 1H NMR and ^{13}C NMR along with their assignments and the molecular structure of the ions.

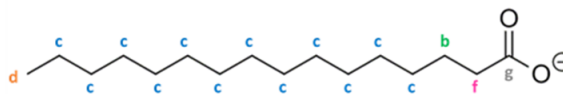
Table 1 Chemical shifts of ^1H NMR for the FAILs.

Protons	$\delta(\text{ppm})$					
	[N ₈₈₈₁][C _{6:0}]	[N ₈₈₈₁][C _{8:0}]	[N ₈₈₈₁][C _{12:0}]	[N ₈₈₈₁][C _{16:0}]	[N ₈₈₈₁][C _{18:0}]	[N ₈₈₈₁][C _{18:1}]
a N-CH ₂	3.4 (m, 6H)	3.37 (m, 6H)	3.4 (m, 6H)	3.37 (m, 6H)	3.4 (m, 6H)	3.3 (m, 6H)
b -CH ₂ -N/ -CH ₂ -O	1.6 (m, 8H)	1.62 (m, 8H)	1.7-1.6 (m, 8 H)	1.62 (m, 8H)	1.6 (m, 8H)	1.6 (m, 8H)
c -CH ₂	1.3 (m, 34H)	1.34-1.24 (m, 38H)	1.40-1.20 (m, 46 H)	1.34-1.24 (m, 54 H)	1.2-1.3 (m, 58H)	1.3 (m, 56H)
d -CH ₃	0.85 (m, 12H)	0.84 (m, 12H)	0.9-0.8 (m, 12 H)	0.84 (m, 12 H)	0.85 (m, 12H)	0.85 (m, 12H)
e N-CH ₃	3.3 (s, 3H)	3.28 (s, 3H)	3.3 (s, 3 H)	3.28 (s, 3H)	3.3 (s, 3H)	3.2 (s, 3H)
f -CH ₂ COO	2.15 (t, 2H)	2.14 (t, 2H)	2.15 (t, 2 H)	2.14 (t, 2H)	2.15 (t, 2H)	2.15 (t, 2H)
g -	-	-	-	-	-	-
h -CH ₂ -CH	-	-	-	-	-	1.95 (m, 4H)
i -CH-CH	-	-	-	-	-	5.3 (t, 2H)

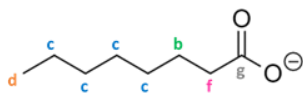
Anions



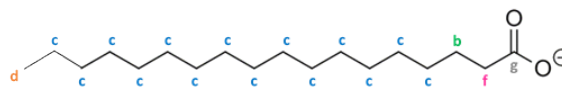
C₆H₁₁O₂⁻ : Hexanoate



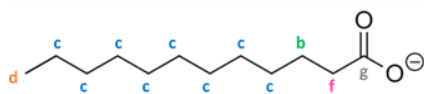
C₁₆H₃₁O₂⁻ : Palmitate



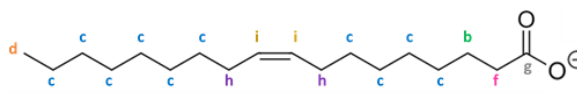
C₈H₁₅O₂⁻ : Octanoate



C₁₈H₃₅O₂⁻ : Stearate



C₁₂H₂₃O₂⁻ : Laurate



C₁₈H₃₃O₂⁻ : Oleate

Cation

C₂₅H₅₄N⁺ : Methyltrioctylammonium

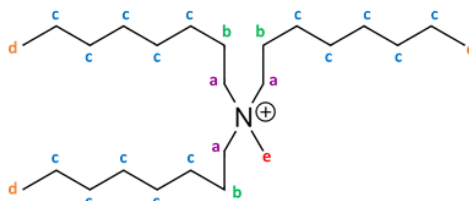


Table 2 Chemical shifts of ^{13}C NMR for the FAILs.

Carbon	$\delta(\text{ppm})$					
	$[\text{N}_{8881}][\text{C}_{6:0}]$	$[\text{N}_{8881}][\text{C}_{8:0}]$	$[\text{N}_{8881}][\text{C}_{12:0}]$	$[\text{N}_{8881}][\text{C}_{16:0}]$	$[\text{N}_{8881}][\text{C}_{18:0}]$	$[\text{N}_{8881}][\text{C}_{18:1}]$
a N-CH ₂	61.34 (3C)	61.2 (3C)	61.16 (3C)	61.2 (3C)	61.19 (3C)	61.3 (3C)
b -CH ₂ -N / -CH ₂ -O	22.4 (4C)	22.3 (4C)	22.3 (4C)	22.3 (4C)	22.3 (4C)	22.3 (4C)
c -CH ₂	22.5-32.2 (17C)	22.5-31.9 (19C)	22.5-31.9 (23C)	22.3-31.9 (27C)	22.5-31.9 (29C)	22.3-31.6 (25C)
d -CH ₃	14-14.1 (4C)	14-14.1 (4C)	14-14.1 (4C)	14-14.1 (4C)	14-14.1 (4C)	14-14.1 (4C)
e N-CH ₃	48.8 (1C)	48.7 (1C)	48.7 (1C)	48.8 (1C)	48.7 (1C)	49 (1C)
f -CH ₂ COO	38.6 (1C)	39.0 (1C)	39.2 (1C)	39.1 (1C)	38.84 (1C)	38.9 (1C)
g -C	179.35 (1C)	179.5 (1C)	179.63 (1C)	179.67 (1C)	179.44 (1C)	179.8 (1C)
h -CH ₂ -CH	-	-	-	-	-	27.1-27.2 (2C)
i -CH-CH	-	-	-	-	-	129.8-129.9 (2C)

On the other hand, Fourier-transform infrared spectroscopy (FTIR) of the FAILs were obtained using a Varian 670-IR FTIR spectrometer with the following experimental setup: 16 scans, 4 cm^{-1} resolution and aperture open. Spectra were recorded between 600 and 4000 cm^{-1} . Finally, Fig. 1 displays the FTIR spectra of the six FAILs.

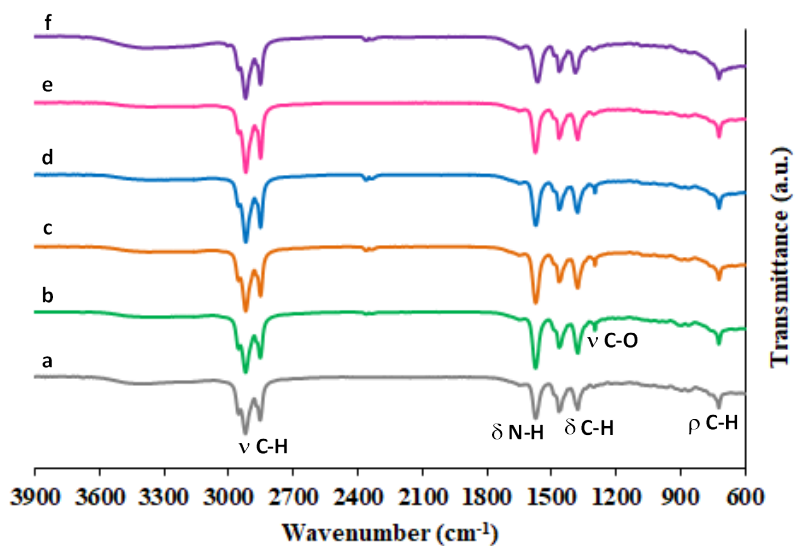


Fig. 1 FTIR spectra of the FAILs including the assignments of the peaks:

a) $[\text{N}_{8881}][\text{C}_{6:0}]$, b) $[\text{N}_{8881}][\text{C}_{8:0}]$, c) $[\text{N}_{8881}][\text{C}_{12:0}]$, d) $[\text{N}_{8881}][\text{C}_{16:0}]$, e) $[\text{N}_{8881}][\text{C}_{18:0}]$ and f) $[\text{N}_{8881}][\text{C}_{18:1}]$.

A commercial ionic liquid provided by Ionic Liquid Technologies GmbH (Io-Li-Tec) sharing the same ammonium-based cation was employed as comparative sample. Table 3 shows the chemical description of the ionic liquids.

Table 3 Chemical description of the FAILs used in this work.

IUPAC name	Acronym	Molecular weight (g/mol)	Empirical formula
Methyltrioctylammonium hexanoate	[N ₈₈₈₁][C _{6:0}]	483	C ₃₁ H ₆₅ NO ₂
Methyltrioctylammonium octanoate	[N ₈₈₈₁][C _{8:0}]	511	C ₃₃ H ₆₉ NO ₂
Methyltrioctylammonium laurate	[N ₈₈₈₁][C _{12:0}]	567	C ₃₇ H ₇₇ NO ₂
Methyltrioctylammonium palmitate	[N ₈₈₈₁][C _{16:0}]	623	C ₄₁ H ₈₅ NO ₂
Methyltrioctylammonium stearate	[N ₈₈₈₁][C _{18:0}]	651	C ₄₃ H ₈₉ NO ₂
Methyltrioctylammonium oleate	[N ₈₈₈₁][C _{18:1}]	649	C ₄₃ H ₈₇ NO ₂
Methyltrioctylammonium bis trifluoromethylsulfonilamide	[N ₈₈₈₁][NTf ₂]	648	C ₂₇ H ₅₄ F ₆ O ₄ N ₂ S ₂

In addition, five different surfaces provided by PCS Instruments were employed in this research for contact angle measurements. Their main mechanical properties are shown in Table 4.

Table 4 Materials of the discs used in wetting tests.

Materials	Roughness*, R _a (μm)	Hardness*
Steel AISI 52100	0.018	225 HV _{0.1}
Aluminum 6082 T6	0.025	116 HV _{0.1}
Tungsten Carbide, 6% Cobalt	0.022	1843 HV _{0.3}
Cast Iron BS1452 grade 240	0.053	225 HV _{0.1}
Bronze PB1 BS 1400	0.027	219 HV _{0.1}

* Measured by authors.

2.2 Wetting properties

Surface tension was measured with a KSV Sigma 700 tensiometer according the Du Noüy's platinum ring method. The temperature measuring system uses a Pt-100 probe and a temperature controller integrated in the system. The Julabo F12-MV water bath used was controlled through a RS-232 port. The temperature readout is in Celsius with 2 decimals and the temperature range was 20-60 °C, which is within the measurement range of the equipment from -5 to 100 °C [54]. The surface tension (γ) measures the free energy of the minimum surface area able to separate liquid and vapor phases. Applying the Gibbs equation [55], the surface tension of a homogeneous liquid linearly decreases with a temperature rise (Eq. 1).

$$\gamma = a - b \cdot T \quad (1)$$

On the other hand, contact angles of the FAILs were measured using a micrometer syringe through the sessile drop methodology in a KSV CAM 200 goniometer [56]. In order to obtain the dynamic advancing contact angle (θ_A), a drop was released at room temperature and recorded through digital images taken in a fixed time interval: first 9 images every half second and next 30 ones every 6 seconds. Besides, the contact angle on both sides (right and left) was calculated through Laplacian methodology. The reference plane is settled in the three-phase line (Fig. 1), so the mathematical methodology is able to calculate the contact angle (θ) using the contact point with the drop for each one of the images taken [57]. The surfaces employed in this test were cleaned, before and after the assay, using acetone in an ultrasonic cleaning bath at room temperature for 5 min, 100 W and then air-dried. Finally, contact angle values reported were obtained from the mean of at least five measurements when steady state was reached (relative error less than 10% on each case). In addition, polarity fraction and spreading parameter were calculated using surface tension and contact angle measurements.

2.3. Wettability determination

Using the Fowkes approach [58], surface tension can be obtained from two different contributions named dispersive (d) and non-dispersive (nd) (Eq. 2). Due to the fact that dispersive interactions are the only ones occurring across the interface, these mentioned interactions (Eqs. 3-5) could be related with the contact angle (θ), the solid-liquid interfacial tension (γ_{SL}) and the adhesion work (W_{SL}), using the Young equation (Eq. 5). Fig. 2 showed the relationship between surface tension (γ) and contact angle (θ), where surface free energy (γ_{SV}) and interfacial tension liquid-vapor (γ_{LV}) are normally indicated as γ_S and γ_L , respectively.

$$\gamma = \gamma^d + \gamma^{nd} \quad (2)$$

$$W_{SL} = 2\sqrt{(\gamma_S^d \cdot \gamma_L^d)} \quad (3)$$

$$\gamma_{SL} = \gamma_S + \gamma_L - W_{SL} \quad (4)$$

$$\gamma_{SL} = \gamma_S - \gamma_L \cdot \cos \theta \quad (5)$$

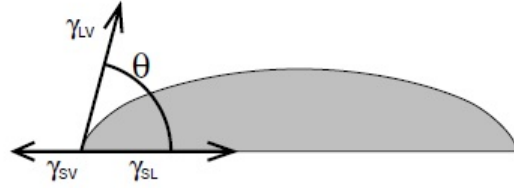


Fig. 2 Surface tension (γ) and contact angle (θ) relationship.

If the surface is homogeneous and flat, interfacial tensions do not change and the contact angle calculated through (Eq. 5) could be assumed constant for a given three-phase system [21]. Finally, contact angle and surface tension could be linked using the previous equations (Eqs. 2-5) in order to obtain a new equation: (Eq. 6).

$$\sqrt{\gamma_S^d \cdot \gamma_L^d} + \sqrt{\gamma_S^{nd} \cdot \gamma_L^{nd}} = 0.5 \cdot \gamma_L (1 + \cos \theta) \quad (6)$$

Because of the two unknown parameters γ_s (non-dispersive and dispersive) appearing in Eq. (6), this formula is insufficient to determine the surface free energy (γ_s) of the solid. Thus, the contact angle has to be measured using at least two test liquids with known values of surface tension components [1], which would yield two equations in the form of the above mentioned Eq. (6). If one phase (liquid or solid) is mostly considered non-polar (dispersive), a good approximation of Eq. (6) is shown in Eq. (7):

$$\gamma_L \cdot (1 + \cos \theta) = 2\sqrt{\gamma_S^d \cdot \gamma_L^d} \quad (7)$$

In order to improve the wettability characterization and considering both surface and liquid effects, Kalin and Polajnar developed a new parameter called Spreading Parameter (SP) [47-49]. New equations (Eqs. 8-9) can be obtained if Young's equation is faced in terms of the difference between free energy of adhesion (W_{SL}), defined in Eq. (5), and free energy of cohesion (W_C), defined in Eq. (10) as the work needed to split isothermally a homogeneous liquid (per unit area).

$$SP = W_{SL} - W_C \quad (8)$$

$$SP = 2\sqrt{\gamma_S^d \cdot \gamma_L^d} + 2\sqrt{\gamma_S^{nd} \cdot \gamma_L^{nd}} - 2\gamma_L \quad (9)$$

$$W_C = 2\gamma_L \quad (10)$$

When $SP > 0$, the contact angle is time-dependent and the liquid spreads completely in order to lower its surface energy (high value of γ_S and a lower value of γ_L). On the other hand, with negative SP values, the liquid forms a spherical equilibrium drop with a given constant contact angle due to cohesion work between ionic liquid molecules being higher than the adhesion work in the solid–liquid interface. Therefore, tribology research should face the knowledge of wettability parameters with the aim of getting a better design of lubrication systems [47-52].

3. Results and discussion

3.1 Surface tension

Average surface tensions of the FAILs and the standard deviation (σ) both obtained from at least 10 measurements of surface tension (γ) and its corresponding temperature (T). Assuming that standard deviation could be the combined standard uncertainty (u_c), the expanded uncertainty (U) is obtained by multiplying u_c by a coverage factor (k). A value of $k=2$ (defining an interval with a level of confidence of approximately 95 %) was chosen to perform the calculations. The results related to surface tension are shown in Table 5.

The surface thermodynamic relationship was analyzed using Gibbs free energy definition (Eq. 1), which states that decreasing the surface area of a mass of liquid is always spontaneous ($G < 0$). Therefore, in order to increase surface area, a certain amount of energy must be added. These data of Table 5 were used to apply Eq. 1 (see Table 6), where the parameter “a” can be allocated to the surface excess energy or enthalpy (E_S), and “b” corresponds to the surface excess entropy (S_S) [50-52]. In addition, Fig. 3 shows the surface tension-temperature relationship of the studied FAILs.

Table 5 Surface tension data of the fatty acid anion-based ionic liquids (FAILs) studied.

$[\text{N}_{8881}][\text{C}_{6:0}]$		$[\text{N}_{8881}][\text{C}_{8:0}]$		$[\text{N}_{8881}][\text{C}_{12:0}]$	
$T \pm \sigma(^{\circ}\text{C})$	$\gamma \pm U(\text{mJ}/\text{m}^2)$	$T \pm \sigma(^{\circ}\text{C})$	$\gamma \pm U(\text{mJ}/\text{m}^2)$	$T \pm \sigma(^{\circ}\text{C})$	$\gamma \pm U(\text{mJ}/\text{m}^2)$
25.879 ± 0.045	24.277 ± 0.078	21.113 ± 0.214	23.989 ± 0.060	23.838 ± 0.361	25.698 ± 0.202
30.051 ± 0.169	24.011 ± 0.040	30.204 ± 0.289	23.599 ± 0.060	31.969 ± 0.077	25.192 ± 0.054
39.933 ± 0.156	23.297 ± 0.030	39.600 ± 0.095	23.022 ± 0.030	40.280 ± 0.137	24.556 ± 0.088
49.937 ± 0.363	22.763 ± 0.052	49.441 ± 0.344	22.485 ± 0.050	49.653 ± 0.048	23.736 ± 0.034
60.321 ± 0.253	22.215 ± 0.072	59.721 ± 0.377	21.927 ± 0.068	59.856 ± 0.266	22.942 ± 0.086
$[\text{N}_{8881}][\text{C}_{16:0}]$		$[\text{N}_{8881}][\text{C}_{18:0}]$		$[\text{N}_{8881}][\text{C}_{18:1}]$	
$T \pm \sigma(^{\circ}\text{C})$	$\gamma \pm U(\text{mJ}/\text{m}^2)$	$T \pm \sigma(^{\circ}\text{C})$	$\gamma \pm U(\text{mJ}/\text{m}^2)$	$T \pm \sigma(^{\circ}\text{C})$	$\gamma \pm U(\text{mJ}/\text{m}^2)$
18.691 ± 0.465	27.984 ± 0.042	20.954 ± 0.118	28.615 ± 0.088	21.073 ± 0.564	28.825 ± 0.126
29.963 ± 0.399	27.118 ± 0.042	30.272 ± 0.278	27.911 ± 0.064	30.091 ± 0.276	27.580 ± 0.048
39.711 ± 0.123	26.419 ± 0.046	39.652 ± 0.093	27.011 ± 0.042	40.100 ± 0.187	26.881 ± 0.078
49.800 ± 0.170	25.550 ± 0.052	49.927 ± 0.143	26.131 ± 0.076	49.959 ± 0.128	26.037 ± 0.038
59.448 ± 0.141	24.770 ± 0.042	60.094 ± 0.187	25.099 ± 0.064	58.843 ± 0.090	25.294 ± 0.040

Table 6 Surface tension measurements of the ionic liquids fitted to Eq. (1).

Ionic liquids	E_s (mJ/m ²)	S_s (mJ/m ² ·K)	Equation ($\gamma = E_s - S_s \cdot T$)	R ²
$[\text{N}_{8881}][\text{C}_{6:0}]$	25.795	0.0602	$25.795 - 0.0602 \cdot T$	0.995
$[\text{N}_{8881}][\text{C}_{8:0}]$	25.179	0.0543	$25.179 - 0.0543 \cdot T$	0.998
$[\text{N}_{8881}][\text{C}_{12:0}]$	27.624	0.0778	$27.624 - 0.0778 \cdot T$	0.997
$[\text{N}_{8881}][\text{C}_{16:0}]$	29.485	0.0789	$29.485 - 0.0789 \cdot T$	0.9991
$[\text{N}_{8881}][\text{C}_{18:0}]$	30.571	0.0900	$30.571 - 0.0900 \cdot T$	0.998
$[\text{N}_{8881}][\text{C}_{18:1}]$	30.528	0.0901	$30.528 - 0.0901 \cdot T$	0.987
$[\text{N}_{8881}][\text{NTf}_2]$	31.805	0.0757	$31.805 - 0.0757 \cdot T$	0.994

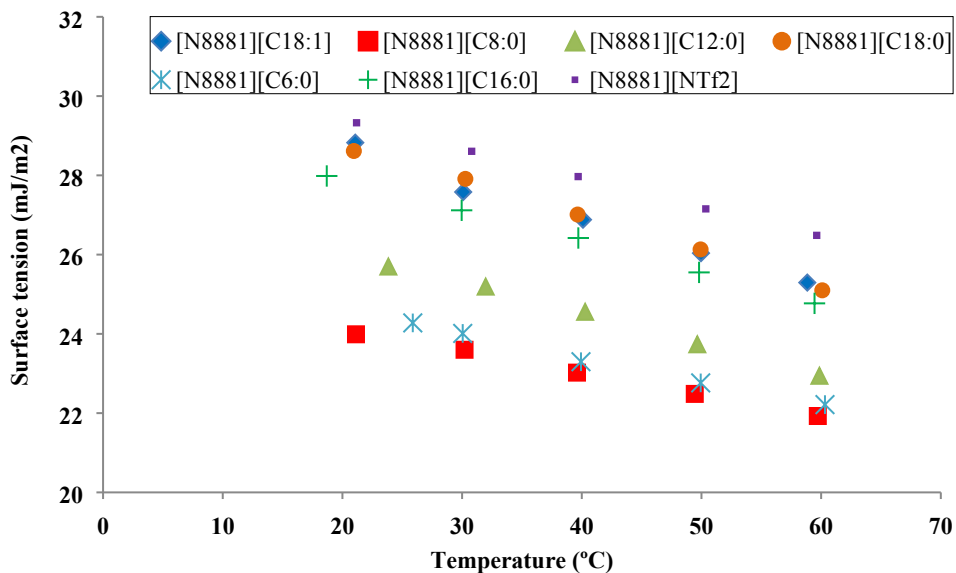


Fig. 3 Temperature- surface tension relationship of fatty acid-based ionic liquids.

Regarding the dependence of the structure of the FAILs on their surface tension, Fig. 4 shows the relation between the length of the chain of the anionic part and the surface tension values at 293 K, calculated using Eq. (1) from experimental results. On viewing these data, the surface tension increases with the chain length. This behavior, which is similar to that of the hydrocarbons reported by Almeida *et. al.* [39], differs from that found for other families of ionic liquids, in which the trend is the opposite **due to the polar contribution to the surface tension** [44, 50, 51].

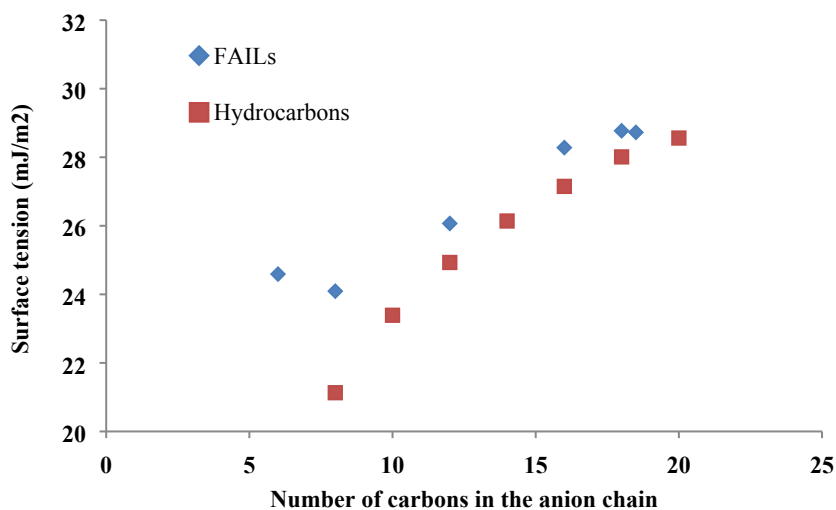


Fig. 4 Structure-surface tension dependence of fatty acid-based ionic liquids and hydrocarbons.

In addition, only the parts of the molecule at the outer surface contribute to the surface tension values, according to the Langmuir's principle [59]. Therefore, the alkyl chain interactions in the studied FAILs should have a main contribution in the surface tension, while the polar groups have a reduced influence. This indicates that in this type of ILs, the surface ordering is mainly **determined** by the aliphatic tails, the contribution of the polar moiety being weak [39]. Unfortunately, a lot of discrepancies exist between sets of data from different sources, mainly attributed to variations on samples purity and possible presence of impurities that have not properly been accounted for [31].

3.2 Contact angle

Fig. 5 shows the variation of contact angle values during 6 different dynamic sessile drop tests (6 liquids in one substrate). With the aim of measuring advancing contact angles, the drop was spread on the surface for approximately 180 seconds. In view of the results, the steady-state is reached early than expected (in about 50 seconds). The behavior on four additional substrates (cast iron, bronze, tungsten carbide and aluminum) was quite similar.

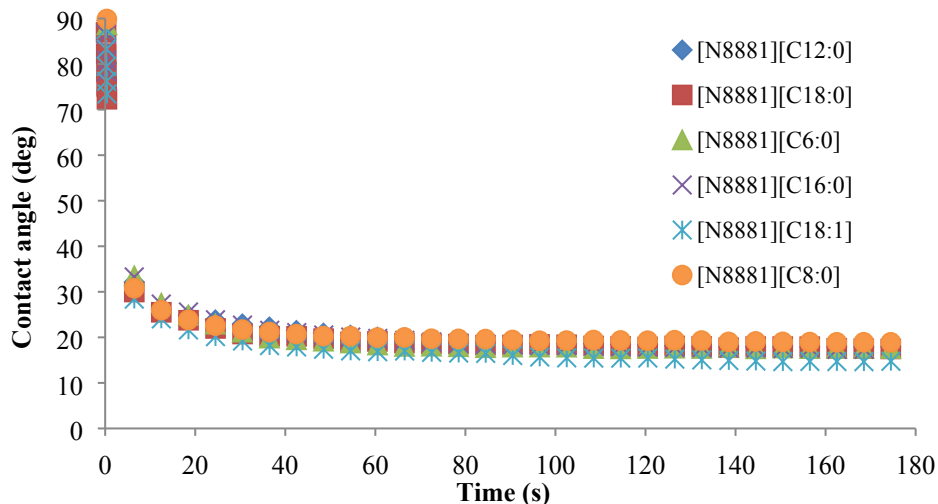


Fig. 5 Advancing contact angle evolution of studied FAILs on the steel surface.

In addition, contact angle measurements using the same dynamic sessile drop assay were conducted with 3 test liquids with known surface tension components (see Table 7), in order to calculate the surface free energy of the 5 substrates employed [60]. The measurements of steady-state contact angle are shown in Table 8.

Therefore, using the data of contact angle from Table 8 with the aim of applying Eq. (6), the values of surface free energy of the five surfaces used in this research are shown in Table 9.

Table 7 Surface tension components of the test liquids found in the literature at 293 K [60].

Test liquids	γ_L (mJ/m ²)	γ_L^d (mJ/m ²)	γ_L^{nd} (mJ/m ²)
Water (W)	72.8	21.8	51.0
Diiodomethane (DIM)	50.8	50.8	-
Ethylene glycol (EG)	48.0	29.0	19.0

Table 8 Steady-state contact angle of the test liquids on five surfaces.

Surface	Water	Diiodomethane	Ethylene glycol
	$\theta \pm \sigma$ (deg)	$\theta \pm \sigma$ (deg)	$\theta \pm \sigma$ (deg)
AISI 52100 Steel	58.150 ± 1.681	42.412 ± 2.026	57.552 ± 0.945
Aluminun	57.100 ± 2.192	45.260 ± 1.134	54.765 ± 1.871
Tungsten Carbide	58.429 ± 3.110	40.068 ± 0.788	43.977 ± 1.669
Cast iron	52.354 ± 2.232	47.570 ± 2.062	61.640 ± 0.848
Bronze	55.649 ± 2.000	41.410 ± 1.247	66.212 ± 0.870

Table 9 Surface free energy (γ_S) of the five surfaces employed.

Surface	γ_S (mJ/m ²)	γ_S^d (mJ/m ²)	γ_S^{nd} (mJ/m ²)
AISI 52100 Steel	52.19	38.38	13.81
Aluminun	52.05	36.87	15.28
Tungsten Carbide	52.92	39.58	13.34
Cast iron	54.18	35.62	18.56
Bronze	54.07	38.89	15.18

On viewing the results from Fig. 5, the steady-state is reached during the advancing sessile drop contact angle experiments. Therefore, the final value of each experiment can be taken as the value of the steady state contact angle. Table 10 displays the mean steady-state contact angle (adding the standard deviation) for all FAILs used on five different surfaces (steel, aluminum, tungsten carbide, cast iron and bronze).

Table 10 Experimental steady-state contact angle measurements of FAILs on different surfaces.

Ionic liquids	Steel	Aluminum	Tungsten Carbide	Cast Iron	Bronze
	$\theta \pm \sigma$ (deg)				
[N ₈₈₈₁][C _{6:0}]	17.626 ± 1.626	18.510 ± 0.713	16.648 ± 1.393	15.398 ± 1.190	16.939 ± 0.333
[N ₈₈₈₁][C _{8:0}]	19.098 ± 1.057	14.458 ± 0.905	15.653 ± 0.675	13.374 ± 0.765	13.673 ± 1.133
[N ₈₈₈₁][C _{12:0}]	19.477 ± 1.623	18.793 ± 1.550	12.134 ± 0.482	19.161 ± 0.811	15.387 ± 0.634
[N ₈₈₈₁][C _{16:0}]	16.840 ± 1.652	14.088 ± 0.660	20.731 ± 1.432	23.933 ± 2.228	12.832 ± 0.070
[N ₈₈₈₁][C _{18:0}]	19.952 ± 1.686	22.807 ± 1.457	27.263 ± 2.685	21.487 ± 1.011	23.663 ± 0.952
[N ₈₈₈₁][C _{18:1}]	16.216 ± 1.441	18.741 ± 1.098	21.517 ± 2.043	18.809 ± 0.979	19.824 ± 1.902

The highest contact angle values were obtained with [N₈₈₈₁][C_{18:0}] for practically all surfaces studied, possibly because of their largest alkyl chain of the anion. On the other hand, [N₈₈₈₁][C_{6:0}] exhibited the more stable contact angle values in all surfaces analyzed in this research, probably related to the contribution of the polar moiety. In addition, because of the novelty of these synthesized fatty acid-based ionic liquids, there is no data of contact angle of these compounds. Besides, contact angle is highly dependent on many parameters, such as purity of the samples, height of needle, drop volume, measuring instrument, etc. [61], which can affect reproducibility. Finally, because of the contact angles obtained with all FAILs and surfaces are time-dependent, it could be claimed that this property cannot be enough to define properly the solid-liquid interaction. With the aim of improving the understanding of wetting behavior, additional parameters such as spreading parameter (defined in Eq. (9)) [47-51, 62] and polarity fraction [50-52, 63, 64] were calculated.

3.3 Polarity fraction

Using ILs as neat lubricants is usually limited due to cost issues, despite the fact that their excellent tribological performance is well known. In order to face this drawback, using ILs as lubricant additive could be the preferable/most suitable choice. However, the feasibility of this promising option is limited by its solubility [13, 14]. Consequently, introducing parameters related to polarity in the characterization of these substances should be helpful with the aim of predicting solubility behavior. From Eq. (2) presented in the section 2.3, a new parameter called polarity fraction (PF) could be presented as the ratio between the polar component (γ_L^{nd}) and the total surface tension (γ_L), Eq. (11).

$$PF = \frac{\gamma_L^{nd}}{\gamma_L} \quad (11)$$

The non-polar component of the surface tension (γ_L^d) was calculated from each surface applying Eq. (7), assuming that the polar component (γ_S^{nd}) is low enough to get a good approximation. Finally, the PF values for each FAIL studied is calculated from Eq. (11). Table 11 summarizes the average results obtained and the standard deviation.

Table 11 Polarity fraction of the FAILs and the test liquids.

	$\gamma_L (mJ/m^2)$	$\gamma_L^d \pm \sigma_C (mJ/m^2)$	$\gamma_L^{nd} (mJ/m^2)$	$PF \pm \sigma_C$
[N ₈₈₈₁][C _{6:0}]	24.591	15.298 ± 0.689	9.293	0.374 ± 0.028
[N ₈₈₈₁][C _{8:0}]	24.093	14.681 ± 0.719	9.412	0.385 ± 0.030
[N ₈₈₈₁][C _{12:0}]	26.068	17.169 ± 0.569	8.899	0.338 ± 0.022
[N ₈₈₈₁][C _{16:0}]	28.281	19.688 ± 0.778	8.593	0.296 ± 0.028
[N ₈₈₈₁][C _{18:0}]	28.771	19.978 ± 1.135	8.793	0.296 ± 0.040
[N ₈₈₈₁][C _{18:1}]	28.726	20.784 ± 1.001	7.942	0.273 ± 0.035
[N ₈₈₈₁][NTf ₂]	28.919*	17.939 ± 1.5563*	10.980*	0.380*
Water	72.8**	21.8**	51.0**	0.708**
Diiodomethane	50.8**	50.8**	0**	0**
Ethylene glycol	48.0**	29.0	19.0**	0.396**

*Data obtained from literature [51].

**Test liquids, data from Table 5.

Due to all FAILs are sharing the same cation, the polarity fraction trend is based on the length of the aliphatic chains of the anion. Therefore, [N₈₈₈₁][C_{6:0}] and [N₈₈₈₁][C_{8:0}] exhibited the highest values of the non-dispersive component of surface tension, with [N₈₈₈₁][C_{16:0}], [N₈₈₈₁][C_{18:0}] and [N₈₈₈₁][C_{18:1}] showing the lowest ones and [N₈₈₈₁][C_{12:0}] exhibiting an intermediate behavior. These results are in agreement with Fig. 4, supporting a polarity fraction-structure relationship: where the polarity fraction is inversely proportional to the number of carbons in the fatty acid anion-based IL.

Comparing the results with the test liquids, FAILs should be considered as moderately polar, similar to ethylene glycol and far away from the typical polar (water) and non-polar (diiodomethane) substances. Regarding the solubility of these FAILs in different base oils, it is expected that those with shorter carbon chain ([N₈₈₈₁][C_{6:0}] and [N₈₈₈₁][C_{8:0}]) should be easily miscible in polar base oils and those with longer carbon chain in the anion

([N₈₈₈₁][C_{16:0}], [N₈₈₈₁][C_{18:0}] and [N₈₈₈₁][C_{18:1}]) should be easily miscible in non-polar base oils. However, additional solubility tests are needed in order to verify this assumption.

3.4 Spreading parameter

Using Eq. (10) presented in the section 2.3, spreading parameter (SP) for 9 different substances (6 FAILs and 3 test liquids) can be easily calculated. Low values of this parameter would indicate that the substance will not spread easily over the surface. If SP is lower than zero, the drop would form an equilibrium sphere with constant contact angle due to the high cohesion work between liquid molecules. Fig. 5 exhibited the main results obtained regarding spreading parameter.

In view of the results, time-dependent contact angle, which means $SP > 0$, happens in 35 liquid – surface possibilities. All of the 6 FAILs showed SP values greater than 20 mJ/m² in all surfaces, and ethylene glycol showed values barely greater than zero. On the other hand, the other 10 liquid-surface combinations (water and diiodomethane on all surfaces) had negative SP values, meaning that drops will not spread over the surface and constant contact angle [47-49]. From a wettability point of view, bronze and cast iron surfaces showed the highest SP values in all cases making them slightly better than the rest. The [N₈₈₈₁][C_{6:0}] and [N₈₈₈₁][C_{8:0}] exhibited the highest values, which is in agreement with the results depicted in Fig. 5 that showed that the shorter alkyl chain length the lower surface tension values and, consequently, an improved wetting behavior.

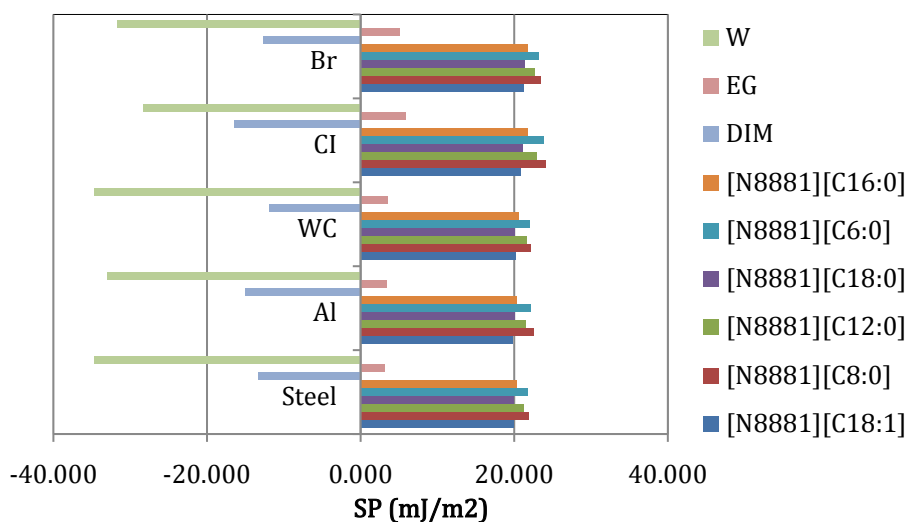


Fig. 6 Spreading parameter values for 9 liquids on 5 surfaces.

3.5 Final remarks

Whenever solid–liquid interface is present in any application, knowing and understanding the wetting behavior through the different wetting parameters faced in this research (spreading parameter, polarity fraction, contact angle and surface tension) are mandatory in order to obtain a proper characterization of the involved phenomena occurring [65-69]. Despite the fact that this wetting study is not always addressed in lubrication science, obtaining different wetting parameters is interesting to design tribology contacts adequately [22, 46, 49-51, 64]. Finally, regarding tribological importance of these wetting parameters with these specific FAILs, it should be noted that:

- Values of the polarity fraction lower than those obtained in the traditional ILs used as lubricant additive, should be interesting in order to get a better solubility of these FAILs in traditional non-polar base oils.
- A positive spreading parameter is recommended in order to get a proper lubrication.

4. Conclusions

Some properties related to the wettability behavior of six fatty acids anion-based ILs: methyltrioctylammonium hexanoate ($[N_{8881}][C_{6:0}]$), methyltrioctylammonium octanoate ($[N_{8881}][C_{8:0}]$), methyltrioctylammonium laurate ($[N_{8881}][C_{12:0}]$), methyltrioctylammonium palmitate ($[N_{8881}][C_{16:0}]$), methyltrioctylammonium stearate ($[N_{8881}][C_{18:0}]$) and methyltrioctylammonium oleate ($[N_{8881}][C_{18:1}]$) on five different surfaces (steel, aluminum, tungsten carbide, cast iron and bronze) were measured or calculated in this research work. From the results obtained, some conclusions can be drawn:

- $[N_{8881}][C_{6:0}]$ and $[N_{8881}][C_{8:0}]$ exhibited the lower surface tension values of the 6 FAILs studied at room temperature. Increasing alkyl chain length caused that surface tension values increased in a similar way that hydrocarbons behavior.
- $[N_{8881}][C_{18:0}]$ exhibited the highest contact angle values in almost all surfaces, possibly because of its longer alkyl chain in the anion moiety.
- Polarity fraction (PF) values varied between 0.273 for $[N_{8881}][C_{18:1}]$ and 0.385 for $[N_{8881}][C_{8:0}]$, these results being in agreement with polarity fraction-structure relationship; where the longer alkyl chain in the anion,

the lower polarity fraction value. These polarity fraction values allowed us to classify this kind of liquids as moderate polar substances.

- All 6 studied FAILs on 5 different surfaces presented values of spreading parameter (SP) between 20-25 mJ/m², indicating that all samples wet all surfaces employed. In addition, bronze and cast iron surfaces exhibited a slightly better wetting behavior than the other surfaces.

Acknowledgments

The authors would like to thank to the Spanish Ministry of Economy and Competitiveness and the Foundation for the Promotion of Applied Scientific Research and Technology in Asturias (FICYT) for supporting this research under the framework of the projects FAILs_LUBEs (DPI2016-79690-R) and LuSuTec (IDI/2018/000131), respectively. The Emulsions and Interfacial Phenomena research group from University of Oviedo is also acknowledged.

Abbreviations

θ	Contact angle	deg
σ	Standard deviation	deg or mJ/m ²
u_c	Combined standard uncertainty	mJ/m ²
U	Expanded uncertainty	mJ/m ²
k	Coverage factor	-
FAIL	Fatty acid ionic liquid	-
NMR	Nuclear magnetic resonance	-
FTIR	Fourier-transform infrared spectroscopy	-
Br	Bronze	-
Al	Aluminum	-
WC	Tungsten carbide	-

CI	Cast iron	-
W	Water	-
DIM	Diiodomethane	-
EG	Ethylen glycol	-
γ_S^d	Dispersive (non-polar) component of surface energy	mJ/m ²
γ_S^{nd}	Non dispersive (polar) component of surface energy	mJ/m ²
γ_{SL}	Solid-liquid interfacial tension	mJ/m ²
$\gamma_L = \gamma_{LV}$	Vapor-liquid interfacial tension	mJ/m ²
E_S	Surface excess energy	mJ/m ²
S_S	Surface excess entropy	mJ/m ² .K
SP	Spreading parameter	mJ/m ²
PF	Polarity fraction	-

References

- [1] Żenkiewicz M. Methods for the calculation of surface free energy of solids. *J Achiev Mater and Manufact Eng* 2007;24:137–45.
- [2] Batchelor T, Cunder J, Fadeev AY. Wetting Study of Imidazolium Ionic Liquids. *J. Colloid Interface Sci.* 2009, 330 (2), 415.
- [3] Guo F, Zhang S, Wang J, Teng B, Zhang T, Fan M. Synthesis and applications of ionic liquids in clean energy and environment: a review, *Curr. Org. Chem.* 19 (5) (2015) 455–468, <https://doi.org/10.2174/1385272819666150114235649>.
- [4] Zhou F, Liang Y, Liu W. Ionic liquid lubricants: designed chemistry for engineering applications, *Chem. Soc. Rev.* 38 (2009) 2590–2599, <https://doi.org/10.1039/b817899m>.
- [5] Berthod A, Ruiz-Ángel MJ, Carda-Broch S. Recent advances on ionic liquid uses in separation techniques. *J Chromatogr A* 2018;1559:2–16. doi:10.1016/j.chroma.2017.09.044.

- [6] Liu H, Yu H. Ionic liquids for electrochemical energy storage devices applications. *J Mater Sci Technol* 2019;35:674–86. doi:10.1016/j.jmst.2018.10.007.
- [7] Ullah Z, Khan AS, Muhammad N, Ullah R, Alqahtani AS, Shah SN, Ghanem OB, Bustam MA, Man Z. A review on ionic liquids as perspective catalysts in transesterification of different feedstock oil into biodiesel. *J Mol Liq* 2018;266:673–86. doi:10.1016/j.molliq.2018.06.024.
- [8] Zhang L, Zhao B, Zhang Y, Zhao Q, Chu H, Liang Z. Advances of ionic liquids-based methods for protein analysis. *TrAC Trends Anal Chem* 2018;108:239–46. doi:10.1016/j.trac.2018.09.008.
- [9] Javed F, Ullah F, Zakaria MR, Akil HM. An approach to classification and hi-tech applications of room-temperature ionic liquids (RTILs): A review. *J Mol Liq* 2018;271:403–20. doi:10.1016/j.molliq.2018.09.005.
- [10] Aghaie M, Rezaei N, Zendehboudi S. A systematic review on CO₂ capture with ionic liquids: Current status and future prospects. *Renew Sustain Energy Rev* 2018;96:502–25. doi:10.1016/j.rser.2018.07.004.
- [11] Wang LY, Guo QJ, Lee MS. Recent advances in metal extraction improvement: Mixture systems consisting of ionic liquid and molecular extractant. *Sep Purif Technol* 2019;210:292–303. doi:10.1016/j.seppur.2018.08.016.
- [12] Amiril SAS, Rahim EA, Syahrullail S. A review on ionic liquids as sustainable lubricants in manufacturing and engineering: Recent research, performance, and applications. *J Clean Prod* 2016. doi:10.1016/j.jclepro.2017.03.197.
- [13] Zhou Y, Qu J. Ionic Liquids as Lubricant Additives – a Review. *ACS Appl Mater Interfaces* 2016;9(4):3209–3222. doi:10.1021/acsami.6b12489.
- [14] Xiao H. Ionic Liquid Lubricants: Basics and Applications. *Tribol Trans* 2016;2004:1–11. doi:10.1080/10402004.2016.1142629.
- [15] Carrera GVSM, Afonso C a M, Branco LC. Interfacial properties, densities, and contact angles of task specific ionic liquids. *J Chem Eng Data* 2010;55:609–15. doi:10.1021/je900502s.
- [16] Alcalde R, García G, Atilhan M, Aparicio S. Systematic Study on the Viscosity of Ionic Liquids: Measurement and Prediction. *Ind Eng Chem Res* 2015;151022154251000. doi:10.1021/acs.iecr.5b02713.

- [17] Shirota H, Mandai T, Fukazawa H, Kato T. Comparison between dicationic and monocationic ionic liquids: Liquid density, thermal properties, surface tension, and shear viscosity. *J Chem Eng Data* 2011;56:2453–9. doi:10.1021/je2000183.
- [18] Zhang X, Huo F, Liu X, Dong K, He H, Yao X, Zhang S. Influence of Microstructure and Interaction on Viscosity of Ionic Liquids. *Ind Eng Chem Res* 2015;54:3505–14. doi:10.1021/acs.iecr.5b00415.
- [19] Hernández Battez A, Bartolomé M, Blanco D, Viesca JL, Fernández-González A, González R. Phosphonium cation-based ionic liquids as neat lubricants: Physicochemical and tribological performance. *Tribol Int* 2016;95:118–31. doi:10.1016/j.triboint.2015.11.015.
- [20] Delcheva I, Ralston J, Beattie DA, Krasowska M. Static and dynamic wetting behaviour of ionic liquids. *Adv Colloid Interface Sci* 2014. doi:10.1016/j.cis.2014.07.003.
- [21] Poleski M, Luczak J, Aranowski R, Jungnickel C. Wetting of surfaces with ionic liquids. *Physicochem Probl Miner Process* 2013;49:277–86. doi:10.5277/ppmp130125.
- [22] Castejón HJ, Wynn TJ, Marcin ZM. Wetting and Tribological Properties of Ionic Liquids. *J Phys Chem* 2014;118:3661–8.
- [23] Shirota H, Mandai T, Fukazawa H, Kato T. Comparison between dicationic and monocationic ionic liquids: Liquid density, thermal properties, surface tension, and shear viscosity. *J Chem Eng Data* 2011;56:2453–9. doi:10.1021/je2000183.
- [24] Ye C, Liu W, Chen Y, Yu L. Room-temperature ionic liquids: a novel versatile lubricant. *Chem Commun (Camb)* 2001:2244–5. doi:10.1039/B106935G.
- [25] Minami I. Ionic liquids in tribology. *Molecules* 2009;14:2286–305. doi:10.3390/molecules14062286.
- [26] Bermúdez MD, Jiménez AE, Sanes J, Carrión FJ. Ionic liquids as advanced lubricant fluids. *Molecules* 2009;14:2888–908. doi:10.3390/molecules14082888.
- [27] Palacio M, Bhushan B. A review of ionic liquids for green molecular lubrication in nanotechnology. *Tribol Lett* 2010;40:247–68. doi:10.1007/s11249-010-9671-8.
- [28] Somers A, Howlett P, MacFarlane D, Forsyth M. A Review of Ionic Liquid Lubricants. *Lubricants* 2013;1:3–21. doi:10.3390/lubricants1010003.
- [29] Hernández Battez A, Fernandes CMCG, Martins RC, Graça BM, Anand M, Blanco D, Seabra JHO. Two phosphonium cation-based ionic liquids used as lubricant additive. Part II: Tribofilm analysis and friction

- torque loss in cylindrical roller thrust bearings at constant temperature. *Tribol Int* 2017;109:496–504. doi:10.1016/j.triboint.2017.01.020.
- [30] Bhattacharjee A, Carvalho PJ, Coutinho JAP. The effect of the cation aromaticity upon the thermophysical properties of piperidinium- and pyridinium-based ionic liquids. *Fluid Phase Equilib* 2014;375:80–8. doi:10.1016/j.fluid.2014.04.029.
- [31] Tariq M, Freire MG, Saramago B, Coutinho JAP, Lopes JNC, Rebelo LPN. Surface tension of ionic liquids and ionic liquid solutions. *Chem Soc Rev* 2012;41:829–68. doi:10.1039/C1CS15146K.
- [32] Ghatee MH, Bahrami M, Khanjari N. Measurement and study of density, surface tension, and viscosity of quaternary ammonium-based ionic liquids ([N222(n)]Tf2N). *J Chem Thermodyn* 2013;65:42–52. doi:10.1016/j.jct.2013.05.031.
- [33] Pereira MM, Kurnia KA, Sousa FL, Silva NJO, Lopes-da-Silva JA, Coutinho JAP, Freire M. Contact angles and wettability of ionic liquids on polar and non-polar surfaces. *Phys Chem Chem Phys* 2015;17:31653–61. doi:10.1039/C5CP05873B.
- [34] Shah SN, Lethesh KC, Mutalib MIA, Pilus RBM. Evaluation of thermophysical properties of imidazolium-based phenolate ionic liquids. *Ind Eng Chem Res* 2015;54:3697–705. doi:10.1021/ie505059g.
- [35] Bhattacharjee A, Lopes-da-Silva JA, Freire MG, Coutinho JAP, Carvalho PJ. Thermophysical properties of phosphonium-based ionic liquids. *Fluid Phase Equilib* 2015;400:103–13. doi:10.1016/j.fluid.2015.05.009.
- [36] Koller TM, Rausch MH, Pohako-esko K, Wasserscheid P, Fröba AP. Surface Tension of Tricyanomethanide- and Tetracyanoborate-Based Imidazolium Ionic Liquids by Using the Pendant Drop Method. *J Chem Eng Data* 2015;60:2665–2673. doi:10.1021/acs.jced.5b00303.
- [37] Bhattacharjee A, Luis A, Santos JH, Lopes-da-Silva JA, Freire MG, Carvalho PJ, Coutinho JAP. Thermophysical properties of sulfonium- and ammonium-based ionic liquids. *Fluid Phase Equilib* 2014;381:36–45. doi:10.1016/j.fluid.2014.08.005.
- [38] Freire MG, Carvalho PJ, Fernandes AM, Marrucho IM, Queimada AJ, Coutinho JAP. Surface tensions of imidazolium based ionic liquids: Anion, cation, temperature and water effect. *J Colloid Interface Sci* 2007;314:621–30. doi:10.1016/j.jcis.2007.06.003.

- [39] Almeida HFD, Freire MG, Fernandes AM, Lopes-da-Silva JA, Morgado P, Shimizu K, Filipe EJM, Canongia Lopes JN, LMNBF Santos, Coutinho JAP. Cation Alkyl Side Chain Length and Symmetry Effects on the Surface Tension of Ionic Liquids. *Langmuir* 2014;30:6408–18. doi:10.1021/la501308q.
- [40] Almeida HFD, Carvalho PJ, Kurnia KA, Lopes-da-Silva JA, Coutinho JAP, Freire MG. Surface tensions of ionic liquids: Non-regular trend along the number of cyano groups. *Fluid Phase Equilib* 2016;409:458–65. doi:10.1016/j.fluid.2015.10.044.
- [41] Bittner B, Wrobel RJ, Milchert E. Physical properties of pyridinium ionic liquids. *J Chem Thermodyn* 2012;55:159–65. doi:10.1016/j.jct.2012.06.018.
- [42] Almeida HFD, Lopes-Da-Silva JA, Freire MG, Coutinho JAP. Surface tension and refractive index of pure and water-saturated tetradecyltrihexylphosphonium-based ionic liquids. *J Chem Thermodyn* 2013;57:372–9. doi:10.1016/j.jct.2012.09.004.
- [43] Almeida HFD, Passos H, Lopes-Da-Silva JA, Fernandes AM, Freire MG, Coutinho JAP. Thermophysical properties of five acetate-based ionic liquids. *J Chem Eng Data* 2012;57:3005–13. doi:10.1021/je300487n.
- [44] Xu A, Wang J, Zhang Y, Chen Q. Effect of alkyl chain length in anions on thermodynamic and surface properties of 1-butyl-3-methylimidazolium carboxylate ionic liquids. *Ind Eng Chem Res* 2012;51:3458–65. doi:10.1021/ie201345t.
- [45] Capelo SB, Méndez-Morales T, Carrete J, López Lago E, Vila J, Cabeza O, Rodríguez JR, Turmine M, Varela LM. Effect of temperature and cationic chain length on the physical properties of ammonium nitrate-based protic ionic liquids. *J Phys Chem B* 2012;116:11302–12. doi:10.1021/jp3066822.
- [46] Schertzer M, Iglesias P. Meta-Analysis Comparing Wettability Parameters and the Effect of Wettability on Friction Coefficient in Lubrication. *Lubricants* 2018;6:70. doi:10.3390/lubricants6030070.
- [47] Kalin M, Polajnar M. The correlation between the surface energy, the contact angle and the spreading parameter, and their relevance for the wetting behaviour of DLC with lubricating oils. *Tribol Int* 2013;66:225–33. doi:10.1016/j.triboint.2013.05.007.
- [48] Kalin M, Polajnar M. The effect of wetting and surface energy on the friction and slip in oil-lubricated contacts. *Tribol Lett* 2013;52:185–94. doi:10.1007/s11249-013-0194-y.

- [49] Kalin M, Polajnar M. The wetting of steel, DLC coatings, ceramics and polymers with oils and water: The importance and correlations of surface energy, surface tension, contact angle and spreading. *Appl Surf Sci* 2014;293:97–108. doi:10.1016/j.apsusc.2013.12.109.
- [50] Blanco D, Bartolomé M, Ramajo B, Viesca JL, González R, Hernández Battez A. Wetting Properties of Seven Phosphonium Cation-Based Ionic Liquids. *Ind Eng Chem Res* 2016;55:9594–602. doi:10.1021/acs.iecr.6b00821.
- [51] Blanco D, Viesca JL, Mallada MT, Ramajo B, González R, Battez AH. Wettability and corrosion of [NTf₂] anion-based ionic liquids on steel and PVD (TiN, CrN, ZrN) coatings. *Surf Coatings Technol* 2016;302:13–21. doi:10.1016/j.surfcoat.2016.05.051.
- [52] Restolho J, Mata JL, Saramago B. On the interfacial behavior of ionic liquids: surface tensions and contact angles. *J Colloid Interface Sci* 2009; 340:82–6. doi:10.1016/j.jcis.2009.08.013.
- [53] Hernández Battez A, Rivera N, Blanco D, Oulego P, Viesca JL, González R. Physicochemical, traction and tribofilm formation properties of three octanoate-, laurate- and palmitate-anion based ionic liquids. *J Mol Liquids* 2019; 284: 639-646. doi: 10.1016/j.molliq.2019.04.050.
- [54] Cambiella A, Benito JM, Pazos C, Coca J, Hernández A, Fernández JE. Formulation of Emulsifiable Cutting Fluids and Extreme Pressure Behaviour. *J. Mater. Process. Technol.* 2007, 184 (1-3), 139.
- [55] Kilaru P, Baker GA, Scovazzo P. Density and surface tension measurements of imidazolium-, quaternary phosphonium-, and ammonium-based room-temperature ionic liquids: Data and correlations. *J Chem Eng Data* 2007;52:2306–14. doi:10.1021/je7003098.
- [56] Tadros TF, Vincent B. Liquid/Liquid Interfaces. *Encyclopedia of Emulsion Technology Vol.1*; Marcel Dekker Inc.: New York, 1983.
- [57] Cabezas MG, Bateni A, Montanero JM, Neumann AW. Determination of Surface Tension and Contact Angle from the Shapes of Axisymmetric Fluid Interfaces without Use of Apex Coordinates. *Langmuir*. 2006, 22 (24), 10053.
- [58] Fowkes FM. Attractive forces at interfaces. *Ind Eng Chem* 1964;56:40–52. doi:10.1021/ie50660a008.
- [59] Langmuir, I. Forces Near the Surfaces of Molecules. *Chem. Rev.* 1930, 6, 451–479.

- [60] Sun C-C, Lee S-C, Hwang W-C, Hwang J-S, Tang I-T, Fu Y-S. Surface Free Energy of Alloy Nitride Coatings Deposited Using Closed Field Unbalanced Magnetron Sputter Ion Plating. *Mater Trans* 2006;47:2533–9. doi:10.2320/matertrans.47.2533.
- [61] Cwikel D, Zhao Q, Liu C, Su X, Marmur A. Comparing contact angle measurements and surface tension assessments of solid surfaces. *Langmuir* 2010;26:15289–94. doi:10.1021/la1020252.
- [62] Lugscheider E, Bobzin K. The influence on surface free energy of PVD-coatings. *Surf Coatings Technol* 2001;142–144:755–60. doi:10.1016/S0257-8972(01)01315-9.
- [63] Restolho J, Mata JL, Saramago B. Choline based ionic liquids: Interfacial properties of RTILs with strong hydrogen bonding. *Fluid Phase Equilib* 2012;322–323:142–7. doi:10.1016/j.fluid.2012.03.016.
- [64] Tiago G, Restolho J, Forte A, Colaço R, Branco LC, Saramago B. Novel ionic liquids for interfacial and tribological applications. *Colloids Surfaces A Physicochem Eng Asp* 2015;472:1–8. doi:10.1016/j.colsurfa.2015.02.030.
- [65] K.R. R, Bontha S, M.R. R, Das M, Balla VK. Laser surface melting of Mg-Zn-Dy alloy for better wettability and corrosion resistance for biodegradable implant applications. *Appl Surf Sci* 2019;480:70–82. doi:10.1016/j.apsusc.2019.02.167.
- [66] Ali N, Zaman H, Bilal M, Shah A-HA, Nazir MS, Iqbal HMN. Environmental perspectives of interfacially active and magnetically recoverable composite materials – A review. *Sci Total Environ* 2019;670:523–38. doi:10.1016/j.scitotenv.2019.03.209.
- [67] Yekeen N, Padmanabhan E, Idris AK, Chauhan PS. Nanoparticles applications for hydraulic fracturing of unconventional reservoirs: A comprehensive review of recent advances and prospects. *J Pet Sci Eng* 2019;178:41–73. doi:10.1016/j.petrol.2019.02.067.
- [68] Smith FR, Brutin D. Wetting and spreading of human blood: Recent advances and applications. *Curr Opin Colloid Interface Sci* 2018;36:78–83. doi:10.1016/j.cocis.2018.01.013.
- [69] Warsinger DM, Chakraborty S, Tow EW, Plumlee MH, Bellona C, Loutatidou S, Karimi L, Mikelonis AM, Achilli A, Ghassemi A, Padhye LP, Snyder SA, Curcio S, Vecitis CD, Arafat HA, Lienhard JH. A review of polymeric membranes and processes for potable water reuse. *Prog Polym Sci* 2018;81:209–37. doi:10.1016/j.progpolymsci.2018.01.004.

Graphical abstract

Fatty acid anion-based
ionic liquids (FAILs)



Wetting properties



Contact angle

